

# Analysis of flow speed distribution in the acoustic streaming generated by two piston sources

## 두 개의 피스톤음원으로부터 발생된 음향유동의 유속분포 해석

Jungsoon Kim,<sup>1</sup> Jihee Jung,<sup>2</sup> and Moojoon Kim<sup>3†</sup>

(김정순,<sup>1</sup> 정지희,<sup>2</sup> 김무준<sup>3†</sup>)

<sup>1</sup>Department of Electrical Engineering, Tongmyong University, <sup>2</sup>General Utility Co. Ltd., Korea,

<sup>3</sup>Department of Physics, Pukyong National University

(Received June 21, 2020; revised August 4, 2020; accepted August 7, 2020)

**ABSTRACT:** To analyze the flow distribution formed by multiple acoustic sources, the distribution of acoustic streaming speed caused by an ultrasonic transducer composed of two identical piezoelectric vibrators was examined for various angles between the sound sources. In order to measure the distribution of the speed along the acoustic axis of the transducer, a simple measurement method using a droplet indicator having density similar to that of water is suggested. The simulation results calculated by a numerical method and experimental results showed a similar tendency, and the change of flow speed distribution with the intersection angle between acoustic beams radiated from two acoustic sources was analyzed.

**Keywords:** Acoustic streaming, Ultrasonic transducer, Multiple acoustic sources, Flow speed distribution, Electroacoustic conversion efficiency

**PACS numbers:** 43.58.Fm, 43.38.Hz

**초 록:** 복수의 음향유동에 의해 형성되는 유속의 분포를 해석하기 위하여 동일한 두 개의 압전진동자로 구성된 초음파 트랜스듀서에 의해 형성되는 음향유동에 대해 음원 사이의 각도에 따른 음향유동속도의 분포를 조사하였다. 거리에 따른 유체입자속도의 분포를 측정하기 위하여 물과 동일한 밀도를 갖는 표시액을 사용한 간단한 측정방법을 제안하였다. 수치해석적인 방법으로 시뮬레이션한 결과와 실험결과는 유사한 경향을 나타내었으며, 두 음원으로부터 방사된 평면파의 방사빔이 교차하는 각도에 따른 음향유동의 속도 분포의 변화를 해석할 수 있었다.

**핵심용어:** 음향유동, 초음파트랜스듀서, 다중음원, 유속분포, 전기음향변환효율

## 1. Introduction

The dynamic effects of ultrasound was widely applied not only to traditional fields such as washing, welding, and humidification, but also to high-tech industries such as therapeutic ultrasound, dispersion of functional nanoparticles, and emulsification of nanoscale.<sup>[1-10]</sup> In particular, the particle manipulation devices such as ultrasonic tweezer have been developed by utilizing the acoustic radiation force and the acoustic streaming effect, which are

the nonlinear phenomenon of ultrasonic waves.<sup>[11-15]</sup>

Recently, we have proposed an efficient dispersion method for nano particles using the shear force of the vortex. The vortex in a fluid is formed by using the ultrasonic streaming effect caused by multiple ultrasonic beams radiated from arrayed ultrasonic transducers in inner surface of a cylinder.<sup>[16]</sup> However, since the angle between the radiation surfaces of piezoelectric vibrators for generating vortices has not been sufficiently studied,

†Corresponding author: Moojoon Kim (kimmj@pknu.ac.kr)

Department of Physice, Pukyong National University, 45, Yongso-ro, Nam-gu, Busan 48513, Republic of Korea

(Tel: 82-51-629-5572, Fax: 82-51-629-5549)



Copyright©2020 The Acoustical Society of Korea. This is an Open Access article distributed under the terms of the Creative Commons Attribution Non-Commercial License which permits unrestricted non-commercial use, distribution, and reproduction in any medium, provided the original work is properly cited.

the design of the shape such as the arrangement of the vibrators is not optimized. Particularly, for designing such an ultrasonic device, it is very important to analyze the distribution of the flow speed depending on the angle between the radiation surfaces of adjacent vibrators and the distance from the sound sources.

In this study, as a basic step, we investigate the change of the acoustic streaming effect generated on the acoustic axis depending on the angle between two piezoelectric vibrators composing an ultrasonic transducer. To measure the flow speed caused by the acoustic streaming, we devise a measurement method using ink droplet with density equivalent to that of water. The measured results are compared with the simulated results.

## II. Theoretical model

Due to the nonlinear terms in the Navier-Stokes equations, harmonic perturbation of the flow will lead to a net time-averaged flow called acoustic streaming.<sup>[17]</sup> Acoustic streaming is a second order (nonlinear) acoustic effect. The time average of acoustic streaming velocity  $\langle \mathbf{v}_2 \rangle$  has the following relations from the second-order perturbation theory.<sup>[18]</sup>

$$\rho_0 \nabla \cdot \langle \mathbf{v}_1 \rangle = -\nabla \cdot \langle \rho_1 \mathbf{v}_1 \rangle, \quad (1)$$

$$\begin{aligned} & \eta \nabla^2 \langle \mathbf{v}_2 \rangle + \beta \eta \nabla (\nabla \cdot \langle \mathbf{v}_2 \rangle) - \langle \nabla p_2 \rangle \\ & = \left\langle \rho_1 \frac{\partial \mathbf{v}_1}{\partial t} \right\rangle + \rho_0 \langle (\mathbf{v}_1 \cdot \nabla) \mathbf{v}_1 \rangle, \end{aligned} \quad (2)$$

Here,  $p_2$  is the second-order pressure. The first-order velocity  $\mathbf{v}_1$  and pressure  $p_1$  are given by the thermodynamic heat transfer equation for temperature  $T_1$ , the kinetic continuity equation, and the dynamic Navier-Stokes equation as follows.

$$\frac{\partial T_1}{\partial t} = D_{th} \nabla^2 T_1 + \frac{\alpha T_0}{\rho_0 C_p} \frac{\partial p_1}{\partial t}, \quad (3)$$

$$\frac{\partial p_1}{\partial t} = \frac{1}{\gamma \kappa} \left[ \alpha \frac{\partial T_1}{\partial t} - \nabla \cdot \mathbf{v}_1 \right], \quad (4)$$

$$\rho_0 \frac{\partial \mathbf{v}_1}{\partial t} = -\nabla p_1 + \eta \nabla^2 \mathbf{v}_1 + \beta \eta \nabla (\nabla \cdot \mathbf{v}_1), \quad (5)$$

Here,  $D_{th}$  is the thermal diffusivity,  $\alpha$  the thermal expansion coefficient,  $\gamma$  the ratio of specific heats,  $\kappa$  the compressibility,  $\eta$  the dynamic viscosity,  $\beta$  the viscosity ratio, and  $T_0$  the ambient temperature, respectively.

## III. Experiment

Two circular piston sound sources with a radius of  $a = 10.0$  mm of Fig. 1 (a) are arranged at an angle  $\theta$ , as shown in Fig. 1 (b). The distance from the origin to the boundary of the circular sound source is  $d = 3.5$  mm. This

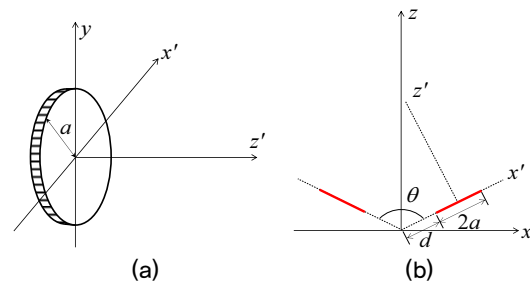


Fig. 1. (Color available online) Circular piston source (a) and array system with two sources (b).

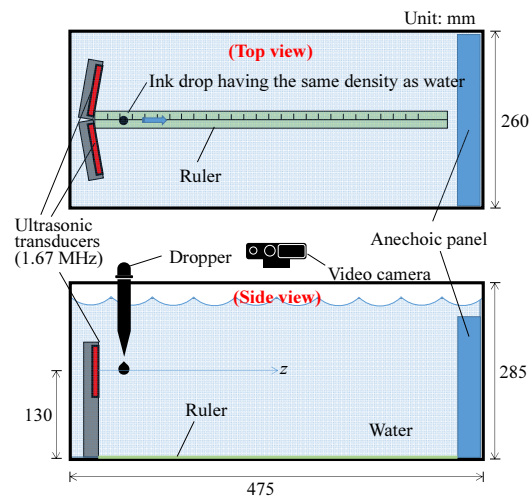


Fig. 2. (Color available online) Experimental setup to measure the flow speed of the acoustic streaming.

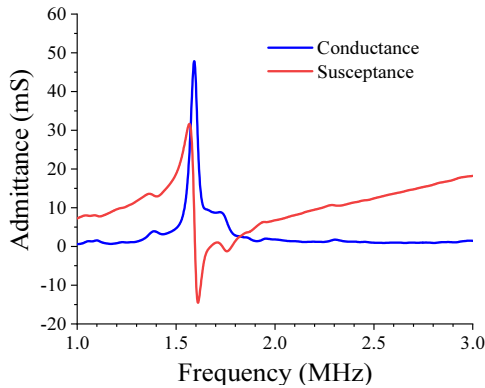


Fig. 3. (Color available online) Resonant characteristic of ultrasonic transducer.

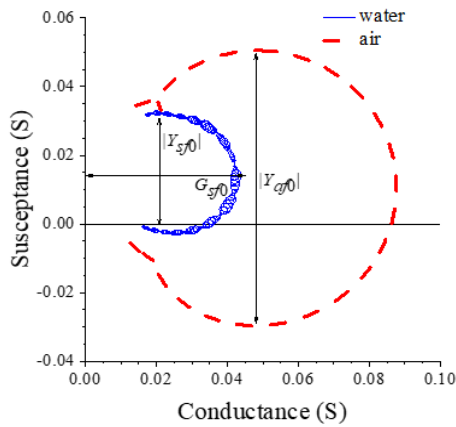


Fig. 4. (Color available online) Admittance loci of ultrasonic transducer for water and air acoustic loads.

array is fixed at the left end of the tank, as shown in Fig. 2. A sound absorbing plate (Eastek, EUA201A) of 10 mm thickness is fixed to the right end and the sound absorption rate of this plate is known as -20 dB above 1 MHz.

In order to examine the characteristics of the piezoelectric vibrator used as a piston source, the input admittance of the transducer was measured and the results are shown in Fig. 3. In this figure, the resonant frequency appeared at about 1.7 MHz, and the value of conductance at resonance was about 50 mS.

To measure the total acoustic energy radiated from the ultrasonic transducer, the electro-acoustic conversion efficiency of the manufactured ultrasonic transducer was measured.

When the acoustic medium is water, the change in the input admittance locus, which varies with and without

acoustic media, was measured, as shown in Fig. 4.

In this figure,  $|Y_{sf0}|$  and  $G_{sf0}$  are the diameter of the admittance locus and the conductance at resonance with the acoustic load, respectively.  $|Y_{af0}|$  is the diameter of the admittance locus without the acoustic load. The measured values of them are as follows.

$$\begin{aligned} |Y_{sf0}| &= 36.27 \text{ mS}, G_{sf0} = 43.74 \text{ mS}, \\ |Y_{af0}| &= 80.14 \text{ mS}. \end{aligned}$$

The electro-acoustic conversion efficiency of the ultrasonic transducer is given by the following equation.<sup>[19,20]</sup>

$$\eta_{ea} = \frac{|Y_{sf0}|}{G_{sf0}} \left( 1 - \frac{|Y_{sf0}|}{|Y_{af0}|} \right). \quad (6)$$

Substituting the above values into Eq. (6), the electro-acoustic conversion efficiency was calculated as  $\eta_{ea} = 45.4\%$ . The circular piezoelectric vibrators used as the piston sources were supplied with an electrical power of  $30.48 \text{ W}_{\text{ms}}$ . From the electro-acoustic conversion efficiency, the acoustic power radiated from the transducer array is therefore estimated as about  $14.0 \text{ W}_{\text{ms}}$ .

In order to measure the flow speed of the acoustic streaming on the  $z$  axis shown in Fig. 1, the droplet of the display liquid, which is an ink droplet diluted with ethanol to have the similar density to that of water in the tank, was released on the axis, as shown in Fig. 2. The ink droplet made a long ink tail along the flow of the acoustic streaming, and moved in a straight line along the axis. The length change of the straight line drawn by the ink was recorded by a video camera. Through the image processing, the length of the line made by the ink at each time was obtained as numerical data, and the instantaneous flow speed of the acoustic streaming was calculated by the numerical differentiation.

## IV. Results and discussions

Fig. 5 shows the results of simulation by the finite

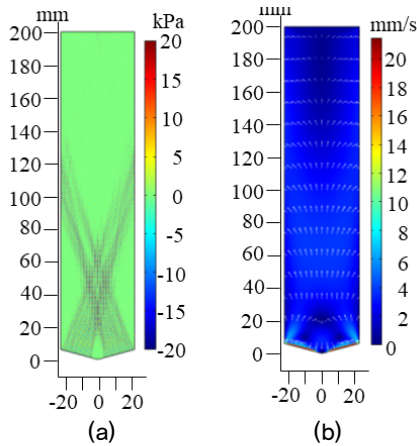


Fig. 5. (Color available online) Simulation results of acoustic field (a) and streaming speed (b) for  $\theta = 150^\circ$ .

Table 1. Physical parameters used in simulation.

Parameters	Symbol	Values
thermal diffusivity	$D_{th}$ (m <sup>2</sup> /s)	$1.46 \times 10^{-7}$
thermal expansion coefficient	$\alpha$ (1/°K)	$2.75 \times 10^{-4}$
ratio of specific heats	$\gamma$	1.01
compressibility	$\kappa$ (1/Pa)	$4.45 \times 10^{-10}$
viscosity ratio	$\beta$	3.16
ambient temperature	$T_0$ (K)	293
density	$\rho_0$ (kg/m <sup>3</sup> )	$9.98 \times 10^2$

element method (commercial COMSOL Multiphysics) when the angle between two piezoelectric vibrators is 150°. Fig. 5(a) and (b) show the acoustic field and the acoustic streaming speed distribution by the arrayed sound sources, respectively. The physical parameters used in the simulation are listed in Table 1.

At this time, proper boundary conditions were imposed on water so that it could be considered as an infinite medium both acoustically and hydrodynamically. Fig. 5(a) shows what the acoustic beams radiated from the two vibrators are crossed each other as the distribution of acoustic pressure, while Fig. 5(b) shows the flow speed distribution of the acoustic streaming caused by the acoustic pressure distribution of Fig. 5(a). The acoustic streaming is generated by the pressure distribution of a large amplitude, and it needs a region to form the acoustic streaming by the nonlinear acoustic effect. Therefore, the maximum region of the flow speed of the acoustic

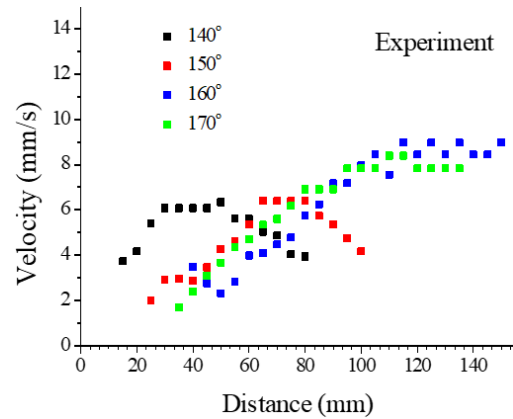


Fig. 6. (Color available online) Experimental result of flow speed distribution of acoustic streaming for different angle between two sound sources.

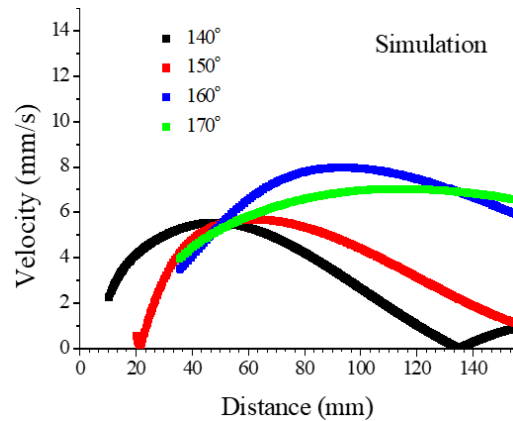


Fig. 7. (Color available online) Simulation result of flow speed distribution of acoustic streaming for different angle between two sound sources.

streaming generally appears after the maximum region of acoustic pressure.<sup>[21]</sup> From Fig. 5, we can see that the maximum flow speed of the acoustic streaming shows at the position of about 50 mm - 80 mm, whereas the maximum acoustic pressure appears at the position of about 30 mm - 50 mm from the sound sources.

The flow speed distributions on the acoustic axis (z-axis in Fig. 1) were obtained for the different angles between the vibrators, as shown in Fig. 6. This result shows that the position of the maximum speed moves as the angle changes, and this tendency is similar to the result of simulation, as shown in Fig. 7. It can be seen from the results of Fig. 7 that the position of the maximum speed of flow is further away from the sound source as the angle

between the two sound sources increases. In this result, as described in the result of Fig. 5, the geometric crossing region of the acoustic beam radiated from the two sound sources does not coincide with the maximum region of the flow speed.

Under the assumption of a near-field, the position of the geometrical intersection of two beams on the acoustic axis can be obtained by the following equation.

$$z = \frac{a+d}{\cos \frac{\theta}{2}}. \quad (7)$$

In the result of Fig. 7, when the angle between the two sound sources is 140°, 150°, and 160°, respectively, the positions of the intersections calculated using Eq. (7) were 39.47 mm, 52.15 mm, and 77.74 mm, respectively away from the transducer, whereas the maximum speed positions for the each angle were 48.11 mm, 62.02 mm and 93.13 mm, respectively. When the angle between the vibrators is 170°, the distance at which the two beams intersect cannot be calculated by applying Eq. (7) because the area is not in the near-field zone.

From the above results, it can be confirmed that the proposed simple method can be applied to measure the speed of acoustic streaming caused by two sound sources, and the tendency of the speed change with the angle between two sound sources is similar in the experiment and the simulation of Fig. 7.

## V. Conclusions

In this study, as a basic step to analyze the acoustic streaming effect caused by multiple ultrasonic beams, the flow speed caused by the acoustic streaming with two identical piezoelectric vibrators was measured.

In order to measure the distribution of flow speed, a measurement method using a colored droplet, as an indicator, was proposed.

The change of the flow speed distribution was measured

for various angles between the two ultrasonic sources. The measurement results showed a similar tendency to the simulation results based on the finite element method.

The results are expected to provide useful information in various of applications using multiple ultrasonic sound sources, such as, non-contact stirring systems, ultrasonic tweezers, and high purity nanoparticle dispersion devices.

## Acknowledgements

This work was supported by the National Research Foundation of Korea (NRF) grant funded by the Korea government (MSIT) (No. 2019R1F1A1062399).

## References

1. G. Clement, J. Sun, T. Giesecke, and K. Hynynen, "A hemisphere array transducer for non-invasive ultrasound brain therapy and surgery," *Phys. Med. Biol.* **45**, 3707-3719 (2000).
2. F. Wu, Z. Wang, H. Zhu, W. Chen, J. Zou, J. Bai, C. Jin, F. Xie, and H. Su, "Feasibility of US-guided high-intensity focused ultrasound treatment in patient-swath advanced pancreatic cancer: initial experience," *Radiology*, **263**, 1034-1040 (2005).
3. E. Constanciel, W. N'Djin, F. Bessiere, F. Chavrier, D. Grinberg, A. Vignot, P. Chevalier, J. Chapelon, and C. Lafon, "Design and evaluation of a transesophageal HIFU probe for ultrasound-guided cardiac ablation: simulation of a HIFU mini-maze procedure and preliminary ex vivo trials," *IEEE Trans. Ultrason. Ferroelectr. Freq. Control*, **60**, 1868-1883 (2013).
4. K. Harada, T. Azuma, T. Inoue, T. Takeo, S. Takagi, Y. Matsumoto, N. Sugita, and M. Mamoru, "Study on high-intensity focused ultrasound focal position control using intracorporeal acoustic device," *Procedia. CIRP* **5**, 290-293 (2013).
5. J. Taurozzi, V. Hackley, and M. Wiesner, "Ultrasonic dispersion of nanoparticles for environmental, health and safety assessment issues and recommendations," *Nanotoxicology*, **5**, 711-729 (2011).
6. X. Li, Y. Yang, and D. Weiss, "Theoretical and experimental study on ultrasonic dispersion of nanoparticles for strengthening cast Aluminum Alloy A356," *Metall. Sci. and Technol.* **26-2**, 12-20 (2008).
7. K. Sato, J. Li, H. Kamiya, and T. Ishigaki, "Ultrasonic dispersion of TiO<sub>2</sub> nanoparticles in aqueous suspension"

- J. Am. Ceram. Soc. **91**, 2481-2487 (2008).
8. C. Lin and L. Chen, "Emulsification characteristics of three- and two-phase emulsions prepared by the ultrasonic emulsification method," *Fuel Process. Technol.* **87**, 309-317 (2006).
  9. C. Lin and L. Chen, "Engine performance and emission characteristics of three-phase diesel emulsions prepared by an ultrasonic emulsification method," *Fuel*, **85**, 593-600 (2006).
  10. S. Nii, S. Kikumoto, and H. Tokuyama, "Quantitative approach to ultrasonic emulsion separation," *Ultrason. Sonochem.* **16**, 145-149 (2009).
  11. T. Kozuka, K. Yasui, T. Tuziuti, A. Towata, and Y. Iida, "Acoustic standing-wave field for manipulation in air," *Jpn. J. Appl. Phys.* **47**, 4336-4338 (2008).
  12. M. Takeuchi, H. Abe, and K. Yamanouchi, "Ultrasonic micromanipulator using visual feedback," *Jpn. J. Appl. Phys.* **35**, 2244-3247 (1996).
  13. J. Lei, P. Glynn-Jones, and M. Hill, "Acoustic streaming in the transducer plane in ultrasonic particle manipulation devices," *Lab. Chip*. **13**, 2133-2143 (2013).
  14. H. Mulvana, S. Cochran, and M. Hill, "Ultrasound assisted particle and cell manipulation on-chip," *Adv. Drug Deliv. Rev.* **65**, 1600-1610 (2013).
  15. S. Liu, Y. Yang, Z. Ni, X. Guo, L. Luo, J. Tu, D. Zhang, and J. Zhang, "Investigation into the effect of acoustic radiation force and acoustic streaming on particle patterning in acoustic standing wave fields," *Sensors*, **17**, 1664 (2017).
  16. M. Kim and J. Kim, "Nanoparticle dispersionizer by ultrasonic cavitation and streaming," *Jpn. J. Appl. Phys.* **57**, 07LE03 (2018).
  17. M. Settnes and H. Bruus, "Forces acting on a small particle in an acoustical field in a viscous fluid," *Phys. Rev. E* **85**, 016327 (2012).
  18. P. Muller, R. Barnkob, M. Jensen, and H. Bruus, "A numerical study of microparticle acoustophoresis driven by acoustic radiation forces and streaming-induced drag forces," *Lab. Chip*, **12**, 4617 (2012).
  19. J. Kim, J. Kim, M. Kim, K. Ha, and A. Yamada, "Arrayed ultrasonic transducers on arc surface for plane wave synthesis," *Jpn. J. Appl. Phys.* **43**, 3061-3062 (2004).
  20. C. H. Sherman and J. L. Butler, *Transducers and Arrays for Underwater Sound* (Springer, New York, 2008), Chap. 12.
  21. T. Kamakura, T. Sudo, K. Matsuda, and Y. Kumamoto, "Time evolution of acoustic streaming from a planar ultrasound source," *J. Acoust. Soc. Am.* **100**, 132-138 (1996).

## Profile

### ▶ Jungsoon Kim (김정순)



She received the B.S. and M.S. degrees from Pukyong National University of Pusan, Korea in 1996 and 1999, respectively and the Ph. D degree from Tokyo University of Agriculture and Technology, Japan in 2002. Since 2006, she has been an assistant professor in Tongmyong University. Her current research interests include ultrasound image, nonlinear acoustics, focused ultrasound, medical ultrasound, and ultrasonic dispersion.

### ▶ Jihee Jung (정지희)



She received the B.S. and M.S. degrees from Pukyong National University of Pusan, Korea in 2013 and 2015, respectively. Since 2019, she has been a researcher of General Utility Co., Ltd, Korea. She has been developed an ultrasonic dispersionizer for nano particles.

### ▶ Moojoon Kim (김무준)



He received the B.S. and M.S. degrees in Applied Physics from Pukyong National University, Busan, Korea in 1985 and 1990, respectively. He got the Ph. D degree in Electric Engineering (major in Ultrasonics) from Tohoku University, Japan in 1994. Since 1997, he has been a professor of the Department of Physics, Pukyong National University. Major research area is ultrasonic transducers. He got the paper presentation award, Japan, from Institute of Electrical Engineers of Japan and the academic award, Korea, from the Acoustical Society of Korea.